ARTICLE TYPE

Influence of applied electric fields on the positive magneto-LC effects observed in the ferroelectric liquid crystalline phase of a chiral nitroxide radical compound

Katsuaki Suzuki, Yoshiaki Uchida, Rui Tamura,* Yohei Noda, Naohiko Ikuma, Satoshi Shimono and Jun Yamauchi

By measuring the electric field dependence of EPR spectra of the ferroelectric liquid crystalline (FLC) phase of (2S,5S)-**1** confined in a surface-stabilized liquid-crystal cell, two magnetic bistable states were observed owing to the anisotropy in spin-spin dipole interactions responsible for the positive 'magneto-LC effects', which refer to the generation of a sort of spin glass-like ferromagnetic interactions (average spin-spin exchange interaction constant $\bar{J} > 0$) induced by weak magnetic fields in the various liquid crystalline (LC) phases of nitroxide radical compound **1**.

1. Introduction

Liquid crystalline (LC) phases are considered to be a sort of 'complexity' system consisting of nonequilibrium dynamic states due to the molecular motion and the coherent collective properties of molecules in the LC state. Therefore, they are sensitive to the external stimuli, such as temperature, pressure, and electric and magnetic fields, or additives like chiral dopants so that the molecular orientation and LC superstructure can easily be altered.[1-4] In this context, there still seems to be challenging and promising perspectives in developing organic soft materials which can show novel complex phenomena in response to external stimuli by making use of an LC environment.

Magnetic liquid crystals have been anticipated to exhibit unique magnetic interactions and unconventional magneto-electric or magneto-optical properties.[5-8] In fact, we observed that all-organic rod-like LC materials with a stable nitroxide radical unit in the central core portion exhibit unique intermolecular ferromagnetic interactions induced by weak magnetic fields in the various LC phases, most likely owing to the swift coherent collective properties of organic molecules with structural anisotropy in the LC state.[9-15] This observation was interpreted in terms of the generation of a sort of spin glass-like inhomogeneous ferromagnetic interactions (the average spin-spin interaction constant, $\bar{J} > 0$) and proved to have nothing to do with the molecular reorientation effects arising from the simple molecular magnetic anisotropy ($\Delta\chi$).[14] We referred to this unique magnetic phenomenon as positive 'magneto-LC effects' ($\bar{J} > 0$).[15]

Among various all-organic magnetic LC compounds synthesized, (2S,5S)-**1** exhibited a chiral smectic C (SmC*) phase between 84.5°C and 36.9°C in the cooling run (Fig. 1a) and showed both the excellent ferroelectric properties in a surface stabilized liquid-crystal cell[16-18] and the explicit ferromagnetic interactions (positive magneto-LC effects, $\bar{J} > 0$) in the bulk SmC* phase.[14] Therefore, it is expected that the unique magneto-
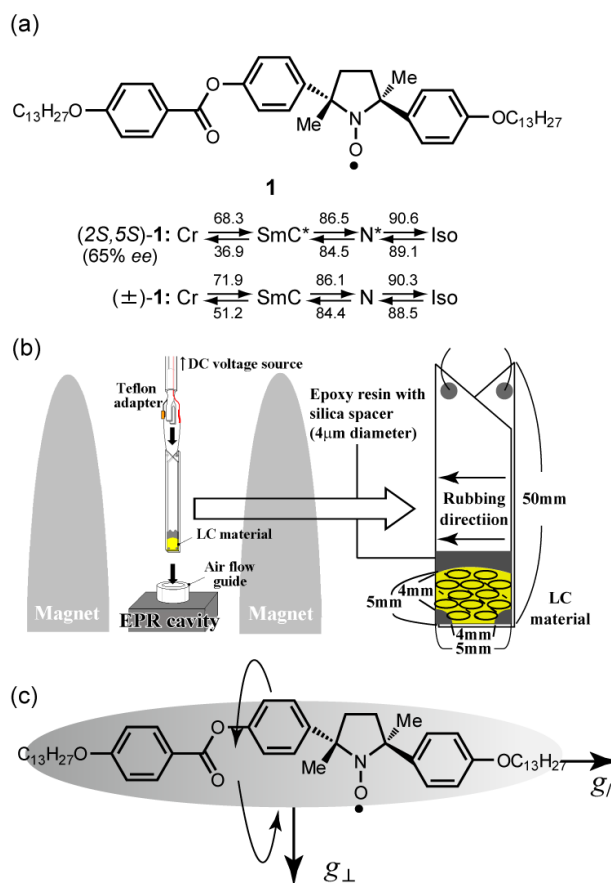

Figure 1. (a) Molecular structure and phase transition temperatures of compound **1**. (b) Experimental setup to monitor the variable-temperature or electric field-dependent EPR spectra of (2S,5S)-**1** confined in a long 4 µm-thick sandwich cell. (c) Principal axes of inertia and g-values ($g_{//}$ and $g_\perp$) of **1**.

electric coupling, which is observed for multiferroic materials possessing both ferroelectric and ferromagnetic properties,[19-21] may occur in the ferroelectric LC (FLC) phase of (2*S*,5*S*)-**1** showing positive-magneto-LC effects. If the magneto-electric coupling were observed for (2*S*,5*S*)-**1**, the resulting magnetic as well as electric bistable states would be utilized to develop magnetic data storage materials operable at ambient temperature.[22,23]

In this article, to clarify the relationship between the ferroelectric properties and positive magneto-LC effects of (2*S*,5*S*)-**1**, we measured the electric field dependence of electron paramagnetic resonance (EPR) spectra of (2*S*,5*S*)-**1** confined in a surface-stabilized liquid-crystal cell and thereby evaluated the EPR parameters such as *g*-value (g), paramagnetic susceptibility (χ_{para}), and the peak-to-peak line width (ΔH_{pp}). It is noteworthy that EPR spectroscopy was found to be a much better means for the measurement of the temperature dependence of χ_{para} for organic nitroxide radical LC compounds at high temperatures than SQUID magnetization measurement,[14,15] because (i) the treatment of the diamagnetic susceptibility (χ_{dia}) term, which is temperature-dependent in LC phases,[24] is unnecessary, (ii) the experimental error is very small even at high temperatures, and (iii) the information on microscopic magnetic interactions such as spin-spin dipole and exchange interactions is directly available.[25]

2. Experimental

(2*S*,5*S*)-**1** was introduced by capillary action into the lower tip (4 mm x 4 mm area) of a handmade long 4 µm-thick sandwich cell (50 mm x 5 mm) in which the inner surfaces of two glass substrates with indium tin oxide (ITO) electrodes were coated with polyimide (Fig. 1b). Only one inner surface in the cell was rubbed horizontally ten times using a velvet roller, because the rubbing of both inner surfaces induced too strong surface anchoring effects so that the ferroelectric switching was fairly disturbed. The use of this cell did not affect the Q-factor seriously. The use of a cylindrical TE011 mode cavity allowed us to disregard the microwave phase and/or Q-factor variations which may arise from the electric-field-induced molecular alignment in the surface-stabilized liquid-crystal cell. The lower tip of the liquid-crystal cell was inserted into the EPR cavity for the following measurement (Fig. 1b).

The temperature or electric field dependence of EPR spectra was measured at a magnetic field of 0.33T. The magnetic data are the mean values of five measurements at each temperature or electric field. Mn^{2+}/MgO was used as a standard. The EPR spectra obtained were Lorentzian in a range of electric fields between +25V and −25V (Fig. S1).

To know whether the application of electric fields produces any artifact on EPR spectra, (±)-**1** which showed an achiral smectic C (SmC) phase between 84.4°C and 51.2°C in the cooling run (Fig. 1a)[14] was loaded on the same thin sandwich cell and the electric field dependence of the EPR spectra was measured between +25V and −25V at 80°C. As expected, no ferroelectric switching was noted and the *g* values were almost constant at 2.0052, showing no electric field dependence (Fig. S2a). Furthermore, no significant change in ΔH_{pp} was noted, too (Fig. S2b). Thus, it has been confirmed that no artifact on EPR spectra is produced by application of electric fields between +25V and −25 V at 80°C.

Methodologically speaking, it should be emphasized that the use of two bistable states enables the interconversion between two molecular orientations by application of electric fields, without rotating the LC cell in the EPR cavity, which would make the accurate evaluation of the change in χ_{para} or ΔH_{pp} difficult. [26,27]

3. Results and discussion

3.1. Polarized Optical Microscopy (POM)

We confirmed the smooth ferroelectric switching in the handmade liquid-crystal cell of (2*S*,5*S*)-**1** by POM at 75 ºC; the dark fan-shaped texture dominated at +25V, indicating the alignment of the molecular long axis parallel to the analyzer (Fig. 2a). By application of an electric field of −25V, the dark texture turned to a light one, in which the molecular long axis is parallel to the rubbing direction but not to either polarizer or analyzer (Fig. 2b).[16] Furthermore, the clockwise rotation of the LC cell by
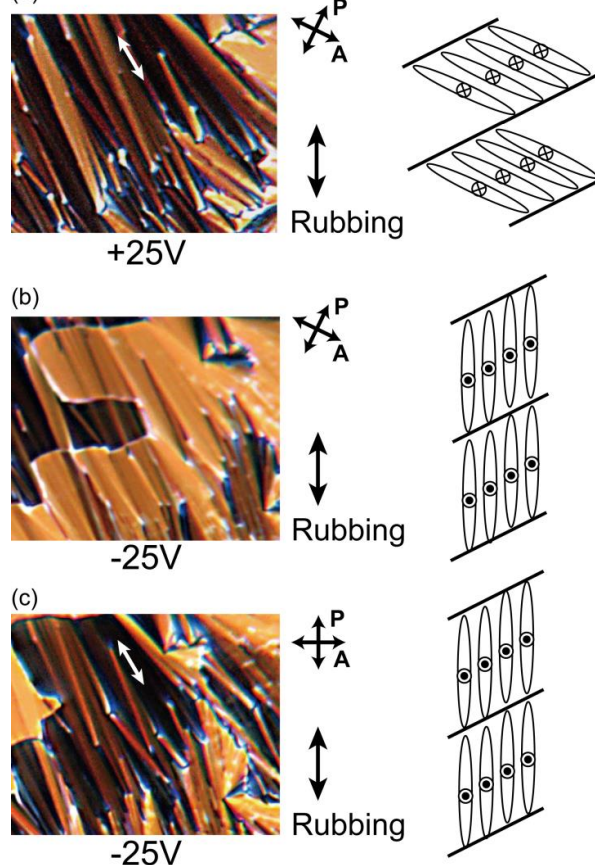

Figure 2. Polarized optical micrographs showing a broken fan-shaped texture in a surface-stabilized thin sandwich cell (4 µm) under homogeneous planar boundary conditions for the ferroelectric LC phase of (2*S*,5*S*)-**1** at 75°C at the electric fields of +25 V and −25V and the corresponding schematic illustration of the direction of the molecular long axes. (a) A dark texture dominated at +25V. (b) A light texture dominated at −25V. (c) A texture observed by rotating the liquid-crystal cell of panel b clockwise by +26° at −25V, followed by rotating the whole photo by −26°. P and A denote the directions of crossed polarizer and analyzer, respectively. White arrows in panels (a) and (c) represent the direction of the layer normal.

+26º at −25V made the molecular long axis parallel to the polarizer and rubbing direction, giving again a dark texture (Fig. 2c). These results indicate that the LC phase of (2S,5S)-**1** in the thin sandwich cell can take two bistable states by changing the polarity of electric field. The tilt angle of (2S,5S)-**1** estimated from POM observation was 31º, which was consistent with the reported value.[16,17]

3.2. EPR Measurement

The sample (2S,5S)-**1** of 65% *ee* was employed because it showed the best ferroelectric behavior between +25 V and −25 V, whereas the samples with higher *ee* values lost the ferroelectric memory effect at 0 V due to its inherently strong winding property in this one-surface rubbed liquid-crystal cell. For the measurement of the temperature dependence of EPR spectra, a magnetic field of 0.33T was applied parallel (Configuration A, Fig. 3a-c) or perpendicular (Configuration B, Fig. 3d-f) to the rubbing direction. For the measurement of the electric field dependence of EPR spectra, after stabilization of the FLC cell by application of AC voltage at 25 V, the electric fields were applied perpendicular ($E \perp H_0$, Fig. 4a-c) or parallel ($E//H_0$, Fig. 4d-f) to the magnetic field at 75°C. We confirmed the reproducibility of these data in Figs. 3 and 4 by repeating the heating and cooling cycle.

3.2.1. Magneto-LC effects in a surface stabilized liquid-crystal cell.

To confirm the generation of the positive magneto-LC effects and the molecular orientation in the surface-stabilized liquid-crystal cell, the temperature dependence of EPR spectra was measured for (2S,5S)-**1** in the cell between 30 and 120°C.

Previously, we reported that χ_{para} could be derived from the Bloch equation[28] by using the EPR parameters, such as *g*, and ΔH_{pp}, and maximum peak height (I'_{m} and $-I'_{\mathrm{m}}$) (eq 1).

$$\chi_{\mathrm{para}} = 2\mu_{\mathrm{B}}gI'_{\mathrm{m}}\Delta H^2_{\mathrm{pp}} / (\sqrt{3}\ h\nu H_1) \qquad (1)$$

where μ_{B} is the Bohr magneton, *h* is Planck's constant, ν is the frequency of the absorbed electromagnetic wave, and H_1 is the amplitude of the oscillating magnetic field.[14,15] Here, the temperature dependence of relative paramagnetic susceptibility ($\chi_{\mathrm{rel,T}}$) is defined as

$$\chi_{\mathrm{rel,T}} = \chi_{\mathrm{para}} / \chi_0 \qquad (2)$$

where χ_0 is the standard value at 30 °C.

Although $\chi_{\mathrm{rel,T}} - T$ plots obeyed the Curie-Weiss law in the Cr phase below 30 °C, the distinct $\chi_{\mathrm{rel,T}}$ increase by 0.27 or 0.28 was noted in case of Configuration A or B, respectively, at the Cr-to-FLC phase transition in the heating run (Fig. 3a and d). The extent of this $\chi_{\mathrm{rel,T}}$ increase was almost identical to that in the bulk sample,[14] strongly suggesting the generation of positive magneto-LC effects in the surface stabilized liquid-crystal cell, too, in which a multi-domain structure is assumed. In the cooling run, the $\chi_{\mathrm{rel,T}}$ increased with decreasing temperature, and abruptly decreased at the FLC-to-Cr phase transition (Fig. 3a and d). Furthermore, the $\chi_{\mathrm{rel,T}}$ increase at the Cr-to-FLC phase transition in the heating run was accompanied by the ΔH_{pp}
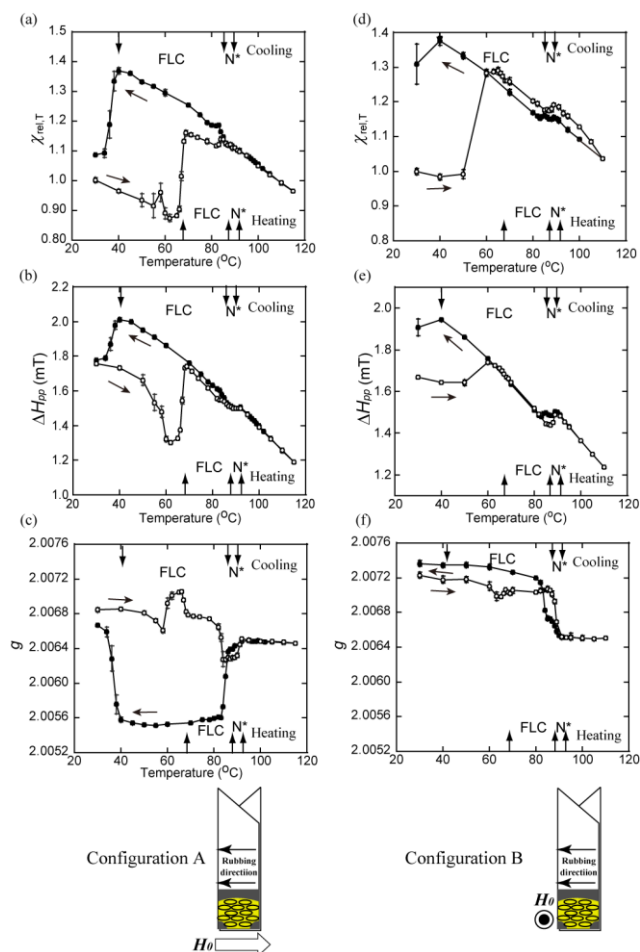

Figure 3. Temperature dependence of (a and d) $\chi_{\mathrm{rel,T,}}$ (b and e) ΔH_{pp}, and (c and f) *g*-value for (2S,5S)-**1** (65% *ee*) confined in a thin rubbed sandwich cell by EPR spectroscopy at a magnetic field of 0.33 T. The magnetic field was applied (a-c) parallel and (d-f) perpendicular to the rubbing direction. The LC temperatures determined by DSC analysis in the heating and cooling runs are shown in the lower and upper sides inside panels, respectively.

increase (Fig. 3b and e), implying the preferential generation of more stable ferromagnetic head-to-tail spin-spin dipole interactions than antiferromagnetic side-by-side ones (see Fig. 5c), as was observed in case of the bulk sample.[14] Non-linear change in ΔH_{pp} and *g*-value in the Cr phase in the heating run is most likely due to the Cr-to-Cr polymorphic transition, which was also observed in the bulk sample.[14]

For the molecular orientation, we could not observe a significant change in the *g*-value in the vicinity of the Cr-to-FLC phase transition temperature in the heating run (Fig. 3c and f). This is most likely due to the strong anchoring effect by the rubbed cell surface. Accordingly, it has been confirmed that the positive magneto-LC effects observed in the liquid-crystal cell have nothing to do with the molecular reorientation effect arising from the simple molecular magnetic anisotropy ($\Delta\chi$). Meanwhile, in the cooling run, the *g*-value in the FLC phase was constant at around 2.0056 or 2.0073 in case of Configuration A or B, respectively (Fig. 3c and f). Since the $g_{//}$ and $g_{\perp}$ values of **1** were previously calculated to be 2.0054 and 2.0068, respectively (Fig. 1c),[29] the experimental *g*-values of 2.0056 and 2.0073 should be attributed to a large contribution of $g_{//}$ and $g_{\perp}$, respectively,

indicating that the molecular long axis is parallel to the rubbing direction and the magnetic field in case of Configuration A, and perpendicular to the magnetic field in case of Configuration B, despite the multi-domain structure.

3.2.2. Electric field dependence of *g*-value in a surface stabilized liquid-crystal cell.

The existence of two bistable states was also confirmed by evaluating the electric field dependence of *g*-value at a magnetic field of 0.33T.

In case of $E \perp H_0$, the *g*-value of (2*S*,5*S*)-**1** exhibited a hysteresis loop between +25V and –25V (Fig. 4a). Upon gradual application of the electric field from +25V to –25V (open circles), the *g*-value of (2*S*,5*S*)-**1** was constant at around 2.0064 (+25V to –2V), then decreased (–2V to –15V), and finally became constant at around 2.0057 (–15V to –25V). Upon reverse application of the electric field from –25V to +25V (closed circles), the *g*-value of (2*S*,5*S*)-**1** was constant at around 2.0057 (–25V to 0V), then increased (0V to +15V), and became constant at around 2.0063 (+15V to +25V). Based on the $g_{//}$ (2.0054) and $g_{\perp}$ (2.0068) of **1** (Fig. 1c),[29] the *g*-value (2.0057) at –25V is most likely to reflect a large contribution of $g_{//}$, suggesting that the molecular long axis of (2*S*,5*S*)-**1** aligns almost parallel to the magnetic field (Fig. 5a). Reduction of the electric field to 0 V did not change the molecular orientation owing to its sufficient ferroelectric memory effect. On the other hand, the *g*-value (2.0063) at +25V indicates that the molecular long axis of (2*S*,5*S*)-**1** is fairly tilted from the direction of the magnetic field (Fig. 5b). Thus, (2*S*,5*S*)-**1** has proved to take two bistable states between +25V and –25V in the surface-stabilized liquid-crystal cell.

In contrast, in case of $E // H_0$, the *g*-value did not show a hysteresis loop between +25V and –25V (Fig. 4d). Since the molecular long axis is almost perpendicular to the applied magnetic field, the *g*-value showed a large contribution of $g_{\perp}$.

3.2.3. Electric field dependence of χ_{para} and ΔH_{pp} in a surface stabilized liquid-crystal cell.

To evaluate the influence of applied electric fields on the positive magneto-LC effects in the FLC phase of (2*S*,5*S*)-**1**, the electric field dependence of the relative paramagnetic susceptibility ($\chi_{rel,E}$), which is defined as

$$\chi_{rel,E} = \chi_{para} / \chi_1 \tag{3}$$

where χ_1 is the standard value at the initial potential of +25V, was plotted.

In case of $E \perp H_0$, the electric field dependence of $\chi_{rel,E}$ showed a hysteresis loop between +25V and –25V (Fig. 4b); the $\chi_{rel,E}$ increased with decreasing *g*-value from 0V to –10V and decreased with increasing *g*-value from 0V to +10V. These results suggest the existence of anisotropy in the magnetic interactions (or the positive magneto-LC effects) in the surface-stabilized liquid-crystal cell.

To gain an insight into the difference in the magnetic interactions between +25V and –25V, the electric field dependence of ΔH_{pp} was compared with that of $\chi_{rel,E}$ (Fig. 4b,c). The ΔH_{pp} drew a hysteresis loop similar to that of $\chi_{rel,E}$.

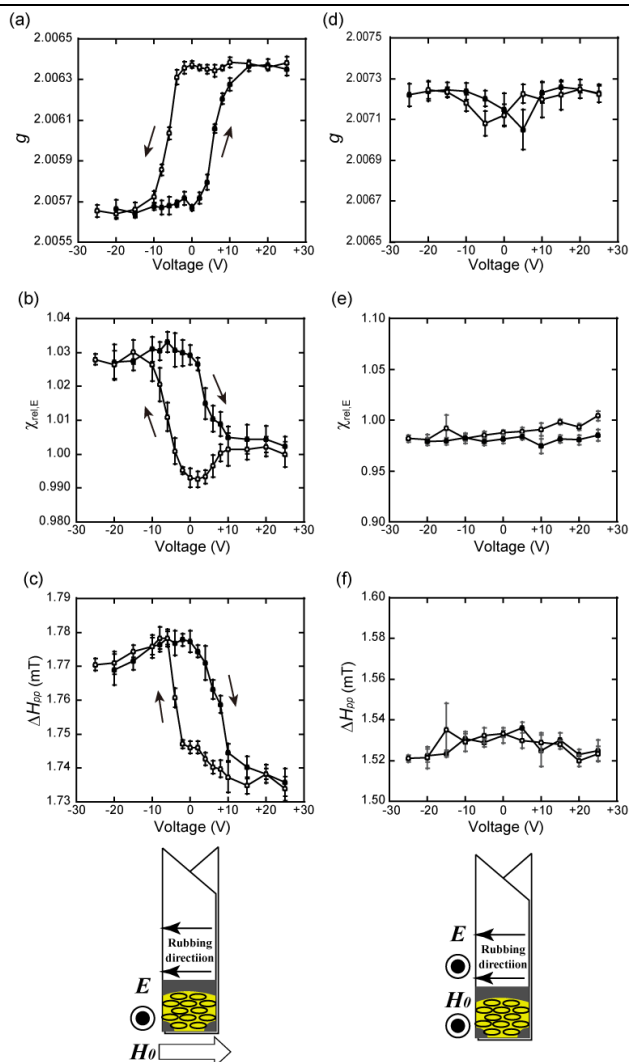The ΔH_{pp} is known to reflect the following two competing

Figure 4. Electric field dependence of *g*-value, $\chi_{rel,E}$, and ΔH_{pp} for the FLC phase of (2*S*,5*S*)-**1** (65% *ee*) confined in a thin rubbed sandwich cell at 75°C by EPR spectroscopy at a magnetic field of 0.33 T. The magnetic field was applied (a-c) perpendicular to the electric field and parallel to the rubbing direction and (d-f) parallel to the electric field and perpendicular to the rubbing direction. Open and filled circles represent the application of electric fields from +25V to –25V and from –25V to +25V, respectively.

factors, (a) spin-spin exchange interaction and (b) spin-spin dipole interaction. If the $\chi_{rel,E}$ change results from the spin-spin exchange interaction, the experimental ΔH_{pp} would decrease with increasing $\chi_{rel,E}$. However, the observed ΔH_{pp} increased or decreased with increasing or decreasing $\chi_{rel,E}$, respectively. This result suggests that the electric field dependence of $\chi_{rel,E}$ should primarily arise from the change in the spin-spin dipole interaction. There are two types of spin-spin dipole interactions; one is a head-to-tail type and the other is a side-by-side type (Fig. 5c).[30] Since the ferromagnetic head-to-tail dipole interaction is energetically more stable than the antiferromagnetic side-by-side dipole interaction and other two, it is easily envisaged that two interacting spins should take different head-to-tail configurations at –25V and +25V in the FLC phase of (2*S*,5*S*)-**1** (Fig. 5a and b); the spin-spin dipole interaction at –25 V was stronger than that at +25V, leading to a higher $\chi_{rel,E}$ value at –25V than that at +25V (Fig. 4b). As the spin-spin dipole interactions contribute to the

(a)

H_0 //
Rubbing direction

−25V

(b)

H_0 //
Rubbing direction

+25V

(c)

U

$\dfrac{2e^2}{r^3}$

$\dfrac{e^2}{r^3}$
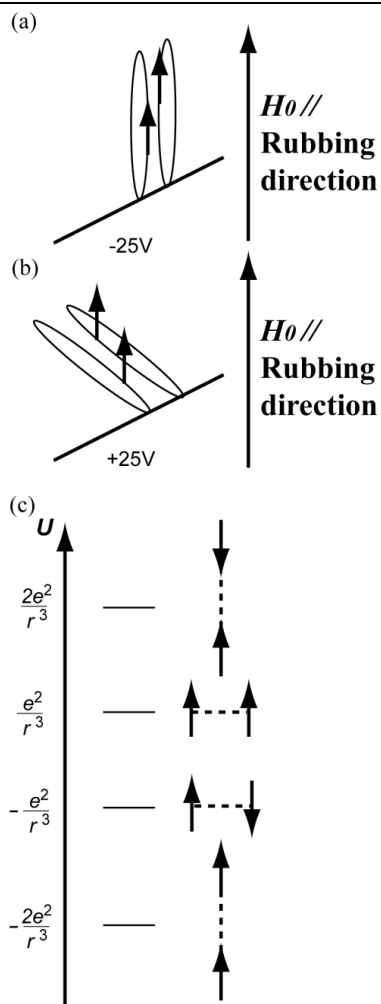
$-\dfrac{e^2}{r^3}$

$-\dfrac{2e^2}{r^3}$

Figure 5. Spin-spin dipole interactions between localized spins in the FLC phase. The molecular long axis is (a) almost parallel to the magnetic field at −25V and (b) tilted from the direction of the magnetic field at +25V; these molecular alignments correspond to panels b and a in Figure 2, respectively. (c) Relative stability of possible four types of spin-spin dipole interactions between two spins.

formation of the spin easy axis,[31] these results have proved the existence of spin easy axis along the molecular long axis in the FLC phase of (2*S*,5*S*)-**1**.

Interestingly, however, the $\chi_{rel,E}$ decreased from +10V to 0V in Fig. 4b. This anomalous behavior cannot be explained simply by either the spin-spin dipole interactions or the molecular reorientation effects, because during the same electric field change the ΔH_{pp} increased and the *g*-value was almost constant (Fig. 4a,c). This ΔH_{pp} increase seems to correspond to the decrease in spin-spin exchange interaction. Although in case of $E \perp H_0$ the *g*-value was constant from +10V to 0V (Fig. 4a), it slightly decreased from 2.0072 to 2.0071 in case of $E//H_0$ during the same electric field change. This result indicates that a molecular or director fluctuation gradually increases in the FLC layer with decreasing electric field, although the overall molecular orientation is maintained even at 0V. This slight molecular fluctuation might be responsible for the anomalous behavior in $\chi_{rel,E}$. Further studies are necessary to clarify this assumption.

In case of $E // H_0$, the $\chi_{rel,E}$ and ΔH_{pp} did not show a hysteresis loop and were almost constant (Figure 4e and f), because the

molecular long axis is always perpendicular to the magnetic field.

4. Conclusions

For the first time we evaluated the influence of the electric fields on the positive magneto-LC effects in the FLC phase of (2*S*,5*S*)-**1** confined in a surface-stabilized liquid-crystal cell by measuring the electric field dependence of the EPR spectra. Consequently, by application of electric fields between +25V and −25V, two magnetic bistable states were observed. The measurement of electric field dependence of ΔH_{pp} indicated that the anisotropy in spin-spin dipole interaction was responsible for the magnetic bistable states; strong spin-spin dipole interactions were observed when the magnetic field was applied parallel to the molecular long axis. Such unique magnetic properties may be applicable to the development of magnetic data storage materials operable at room temperatures.

Furthermore, we observed an anomalous magnetic behavior during the electric field change from +10V to 0V, which can be explained by the slight molecular fluctuation occurring under low electric fields. This anomalous magnetic behavior may be regarded as a sort of magneto-electric coupling in the FLC state. To gain a deep insight into the magneto-LC-effects and prove the existence of this magneto-electric coupling, the combined use of molecular dynamics simulation and quantum chemical calculation would be very effective. Such an in-depth understanding of positive magneto-LC effects would open up a new research field in the development of totally new all-organic magnetic LC materials.

Acknowledgements

Supporting Information Available: Figure S1 and S2.

References

Graduate School of Human and Environmental Studies, Kyoto University, Kyoto, 606-8501, Japan. Fax: +81 75-753-7915; Tel: +81 75-753-6815; E-mail: tamura.rui.8c@kyoto-u.ac.jp

1   S. Chamdrasekhar (ed), *Liquid Crystal Second Edition*, Cambridge University Press, Cambridge, 1992.
2   D. Demus, J. Goodby, G. W. Gray, H.-W. Spiess, V. Vill (ed), *Physical Properties of Liquid Crystals*, Wiley-VCH, Weinheim, 1999.
3   I. Dierking, *Textures of Liquid Crystals*, Wiley-VCH, Weinheim, 2003.
4   L. M. Bilinov, *Electro-Optical and Magneto-Optical Properties of Liquid Crystals*, John Wiley & Sons, New York, 1983.
5   P. M. Lahti (ed), *Magnetic Properties of Organic Molecules*, Marcel Dekker, New York, 1999.
6   J-L. Serrano, *Metallomesogens: Synthesis, Properties, and Applications*, Wiley-VCH, Weinheim, 1996.
7   K. Binnemans, C. Görller-Walrand, *Chem. Rev.* 2002, **102**, 2303.
8   N. E. Domracheva, I. V. Ovchinnikov, A. N. Turanov, V. N. Kostantinov, *J. Magn. Magn. Mater.*, 2004, **269**, 385.

9   G. I. Likhtensthtein, J. Yamauchi, S. Nakatsuji, A. I. Smirnov, R. Tamura, *Nitroxide*: *Applications in Chemistry, Biochemistry, and Materials Science*, Wiley-VCH, Weinheim, 2008.

10 R. Tamura, Y. Uchida, K. Suzuki, in *Liquid Crystals Beyond Displays: Chemistry, Physics, and Applications,* ed. Q. Li, John Wiley & Sons, Hoboken, 2012, pp. 83-110.

11 R. Tamura, Y. Uchida, K. Suzuki, in *Nitroxides: Theory, Experiment and Applications*, ed. A. I. Kokorin, InTech, Croatia, 2012, pp. 191-210.

12 R. Tamura, Y. Uchida, N. Ikuma, *J. Mater. Chem*., 2008, **18**, 2872.

13 Y. Uchida, N. Ikuma, R. Tamura, S. Shimono, Y. Noda, J. Yamauchi, Y. Aoki, H. Nohira, *J. Mater. Chem*., 2008, **18**, 2950.

14 Y. Uchida, K. Suzuki, R. Tamura, N. Ikuma, S. Shimono, Y. Noda, J. Yamauchi, *J. Am. Chem. Soc*., 2010, **132**, 9746.

15 K. Suzuki, Y. Uchida, R. Tamura, S. Shimono and J. Yamauchi *J. Mater. Chem.,* 2012, **22**, 6799.

16 N. Ikuma, R. Tamura, S. Shimono, Y. Uchida, K. Masaki, J. Yamauchi, Y. Aoki, H. Nohira, *Adv. Mater*., 2006, **18**, 477.

17 N. Ikuma, R. Tamura, K. Masaki, Y. Uchida, S. Shimono, J. Yamauchi, Y. Aoki, H. Nohira, *Ferroelectrics*, 2006, **343**, 119.

18 R. Kogo, F. Araoka, Y. Uchida, R. Tamura, K. Ishikawa, H. Takezoe, *Appl. Phys. Express*, 2010, **3**, 041701.

19 W. Erenstein, N. D. Mathur, J. F. Scott, *Nature*, 2006, **442**, 759.

20 C. N. R. Rao, C. R. Serrao, *J. Mater. Chem*., 2007, **17**, 4931.

21 C. Felser, G. H. Fecher, B. Balke, *Angew. Chem. Int. Ed*., 2007, **46,** 668.

22 J. Veciana and I. Ratera, in *Stable Radicals: Fundamentals and Applied Aspects of Odd-Electron Compounds*, ed. R. G. Hicks, John Wiley & Sons, Chichester, 2010, pp. 33-80.

23 I. Ratera and J. Veciana, *Chem. Soc. Rev*., 2012, **41**, 303.

24 H. J. Müller, W. Haase, *J. Phys. (Paris)*, 1983, **44**, 1209.

25 Y. Uchida, K. Suzuki, R. Tamura, *J. Phys. Chem. B*, 2012, **116**, 9791.

26 Y. Noda, S. Shimono, M. Baba, J. Yamauchi, N. Ikuma, R. Tamura, *J. Phys. Chem. B*., 2006, **110**, 23683.

27 Y. Noda, S. Shimono, M. Baba, J. Yamauchi, Y. Uchida, N. Ikuma, R. Tamura, *Appl. Magn. Reson*., 2008, **33**, 251.

28 F. Bloch, *Phys. Rev.,* 1946, **70**, 460.

29 Y. Uchida, R. Tamura, N. Ikuma, S. Shimono, J. Yamauchi, Y. Shimbo, H. Takezoe, Y. Aoki, H. Nohira, *J. Mater. Chem*., 2009, **19,** 415.

30 J. A. Weil, J. R. Bolton, *Electron Paramagnetic Resonance-Elementary Theory and Practical Application Second Edition*, John Wiley & Sons, Hoboken, 2007.

31 T. Kawamoto and N. Suzuki, *J. Phys. Soc. Jpn*., 1993, **63**, 3158.